Microstructure evolution and mechanical properties of rheo-squeeze casting AZ91-Ca alloy during heat treatment

***Yang Zhang[1], Xiao-ping Li [1], Shun-ping Sun [1], Ya-lin Lu [1], and Guo-hua Wu [2]**

1. School of Materials Engineering, Jiangsu University of Technology, Changzhou 213001, China

2. National Engineering Research Center of Light Alloy Net Forming, Shanghai Jiao Tong University, Shanghai 200240, China

Abstract: The rheo-squeeze casting (RSC) process is a newly-developed casting process for high-performance components. In order to further improve the mechanical properties of magnesium alloys, AZ91-2wt.%Ca (AZX912) alloy was prepared by the RSC process and then subjected to heat treatment. The microstructure evolution and mechanical properties of AZX912 alloy during heat treatment were investigated. It was found that during solid solution treatment at 410 °C, β-$Mg_{17}Al_{12}$ phase with low melting point dissolves into α-Mg matrix, while the connected network-like Al_2Ca phase with high melting point tends to separate gradually, and the tips of Al_2Ca phase is partially spheroidized. With the increase of solid solution time, the yield strength (YS) of AZX912 alloy decreases gradually while the ultimate tensile strength (UTS) and elongation to failure (E_f) increase continuously. Isothermal ageing at 225 °C promotes the precipitation of β-$Mg_{17}Al_{12}$ phase in the matrix of AZX912 alloy. The hardness reaches the peak after ageing for 96 h and the increase in hardness is about 24.8%. The precipitation of β-$Mg_{17}Al_{12}$ phase during ageing treatment is beneficial to YS but harmful to E_f. The mechanism of microstructure evolution during heat treatment and its effect on mechanical properties are discussed.

Key words: magnesium alloys; semisolid processing; heat treatment; microstructure; mechanical properties

CLC numbers: TG146.22 **Document code:** A **Article ID:** 1672-6421(2017)06-485-07

Among existing commercial Mg alloys, Mg-9Al-1Zn(wt.%) (AZ91) alloy is widely used in automobile, electronic and aviation industries. The addition of Ca element is able to further improve the creep resistance and ignition proof behavior of AZ91 alloy [1-2]. With the addition of Ca, the amount of unstable β-$Mg_{17}Al_{12}$ phase decreases and Ca-containing phases with high melting point form in the AZ91-Ca alloys. Meanwhile, the addition of Ca can promote the formation of compact oxide film in the melt and protect it from severe oxidation during the melting and casting process [2-4]. Therefore, AZ91-Ca alloy is thought to be a promising heat-resistant and ignition-proof Mg alloy. However, when the content of Ca element in AZ91 alloy exceeds 1wt.%, the tensile properties of the alloy at ambient temperature deteriorates severely, which is a main obstacle to its practical application [5].

***Yang Zhang**

Male, born in 1988, Lecturer, Ph. D. His research interests mainly focus on the semi-solid processing of Mg alloys and super-light Mg-Li alloys. To date, he has published more than 10 papers.

Email: zhangyang@jsut.edu.cn

Received: 2017-02-27; Accepted: 2017-06-28

As a potential near net shape technique to manufacture components with high performance, rheo-forming has gained increasing attentions in past decades [6]. In rheo-forming process, the prepared semisolid slurry is mostly shaped by die casting or squeeze casting. Since the mould filling of die casting is achieved under relatively high speed, the elimination of porosity is scarcely possible. In contrast, the mould filling rate in rheo-squeeze casting (RSC) is low and the solidification of prepared semisolid slurry is finished under applied pressure all along. Therefore, compared to rheo-die casting (RDC), components prepared by RSC process is likely to exhibit better comprehensive mechanical properties due to its lower porosity level and better integrity. Wu et al. carried out a systematic study on RSC process of Al alloys (including A356, 2024, 7075, etc.) and found that the mechanical properties of Al alloys prepared by RSC process were much better than samples prepared by conventional casting process [7-9]. Moreover, owing to the low porosity level, components made by RSC can be subjected to subsequent heat treatment. For example, Mahathaninwong et al. proved that T6 heat treatment could further improve the mechanical properties of RSC 7075 Al alloy [10].

Up to now, the microstructure evolution and mechanical properties of AZ91 alloy during heat treatment has been investigated extensively. During solid solution treatment, β-$Mg_{17}Al_{12}$ phase would dissolve into α-Mg matrix and results in super-saturated α-Mg phase. In the subsequent ageing treatment, β-$Mg_{17}Al_{12}$ phase precipitates from the super-saturated α-Mg phase. It is also found that the addition of Ca can influence the precipitation behavior of AZ91 alloy and inhibit the harmful discontinuous precipitation [11]. Besides, the increase of Ca content changes the phase constitution of AZ91-Ca alloys in the as-cast state [12]. For example, in AZ91-2wt.%Ca alloy, Al_2Ca phase is the dominant second phase rather than β-$Mg_{17}Al_{12}$ phase [13]. Its microstructure evolution and precipitation behavior during heat treatment is different from AZ91 alloy definitely. However, previous studies mainly focused on the heat treatment of AZ91-Ca alloy with a low Ca content (≤1wt.%) [14], while the AZ91-Ca alloy with a high Ca content (≥2wt.%) was scarcely investigated.

In present work, AZ91-2wt.% alloy (AZX912) is prepared by the RSC process and then subjected to heat treatment. The effects of solid solution and isothermal ageing on microstructure evolution and mechanical properties of AZX912 alloy were investigated. The mechanism of microstructure evolution during heat treatment and its effect on mechanical properties were discussed.

1 Experimental procedure

AZX912 alloy was prepared with AZ91D alloy ingots and pure Ca (99.9wt.%). Under the mixed protection atmosphere of SF_6 (1vol.%) and CO_2 (99vol.%), the pre-weighed AZ91D ingot was heated and melted. When the temperature of AZ91D melt reached 700 °C, pure metal Ca was added. Then the melt was stirred for 3 min to ensure the dissolution and homogeneous distribution of Ca. Then the melt was heated to 700 °C again and held at 700 °C to be prepared for the further preparation of semi-solid slurry. Inductively coupled plasma analyzer (ICP) was used to determine the chemical composition of AZX912 alloy and the actual chemical composition was determined to be Mg-8.21Al-0.53Zn-0.20Mn-1.76Ca (wt.%).

The details of the RSC process of AZX912 alloy were demonstrated in Ref. [15]. In this study, gas flow was set as 6 L•min^{-1}, the pouring temperature of semisolid slurry was 596 °C and applied pressure used for the RSC process was 120 MPa. The size of cast samples was Φ55×80 mm. The melting point of β-$Mg_{17}Al_{12}$ phase is 437 °C. In order to prevent over-burn, 410 °C is often used as solid solution temperature for AZ91 alloy. In this study, the temperature for solid solution treatment was also set as 410 °C and held for up to 64 h followed by quenching in cold water. The temperature for ageing treatment is in the range of 200–250 °C. Therefore, specimens after solid solution treated at 410 °C for 64 h were aged at 225 °C in oil bath up to 224 h.

Specimens for microstructure characterization were cut from the samples and prepared with standard metallographic procedures. Optical microscopy (OM, ZEISS Axio observer A1), scanning electron microscopy (SEM, Quanta FEG 250, equipped with EDS) and transmission electron microscopy (TEM, JEM-2100) methods were used for microstructure characterization. Quantitative image analysis software (Imagepro-plus 6.0) was used for metallographic analysis. X-ray diffraction (XRD, D/max 2550VL/PC) using Ni-filtered Cu-Kα radiation was used for phase constitution characterization. A Vickers hardness testing machine was used to measure the age hardening behavior during ageing treatment, under a load of 49 N and a holding time of 20 s. Ambient temperature tensile testing was done according to ISO6892-1:2009. Rectangular tensile specimens with a gauge length of 10 mm were cut from the samples. Zwick/Roell-20 kN material test machine was used for ambient temperature tensile testing and the cross-head speed was 1 mm•min^{-1}.

2 Results and discussion

Figure 1 shows XRD patterns and analysis results of AZX912 alloy under different T4 treatment conditions. According to XRD results, as-cast RSC AZX912 alloy contains α-Mg, β-$Mg_{17}Al_{12}$ and Al_2Ca phases. After T4 treatment at 410 °C for 32 h, β-$Mg_{17}Al_{12}$ phase with low thermal stability almost dissolves into α-Mg matrix, which is confirmed by the disappearance of its diffraction peaks. Meanwhile, the diffraction peaks of Al_2Ca phase remains, indicating that Al_2Ca phase with high melting point could not dissolve into α-Mg matrix at 410 °C. It is also found in Fig. 1 that a further increase in the holding time for T4 treatment to 64 h shows little difference in XRD patterns. These results prove that the extended solution time has little influence on phase constitution of AZX912 alloy.

Figure 2 shows the microstructures of AZX912 alloy under different T4 treatment conditions. Due to the discontinuous solidification pathway of the RSC process, the second phases distribute uneven in the as-cast AZX912 alloy and most of them aggregate in the residual melt. It is observed that two kinds of second phases coexist in as-cast AZX912 sample, as shown in Fig. 2(b). The irregularly block-like phase is β-$Mg_{17}Al_{12}$ phase and the lamellar-like phase is Al_2Ca phase. After T4 treatment

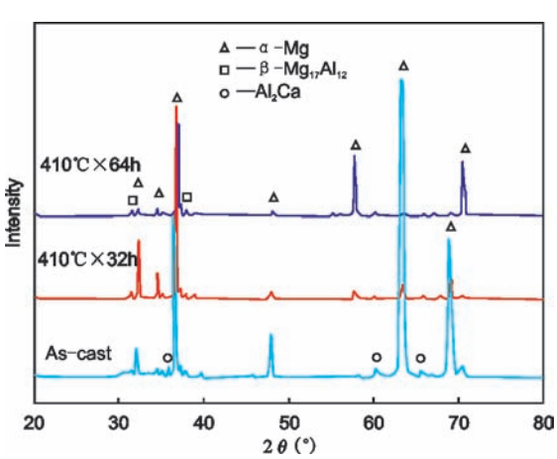

Fig. 1: XRD patterns and analysis results of AZX912 alloy under as-cast and different T4 treatment conditions

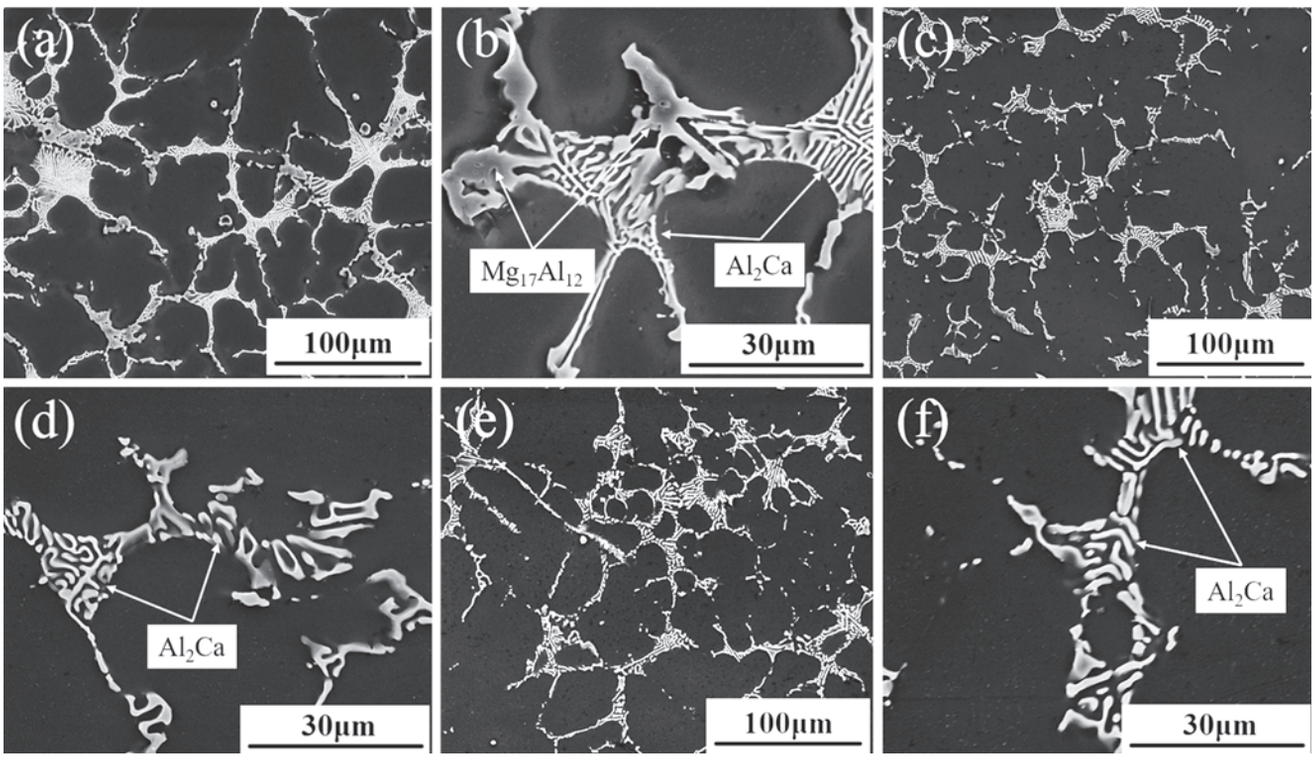

Fig. 2: SEM images of AZX912 alloy under different T4 treatment conditions: (a, b) as-cast; (c, d) 410 °C × 32 h and (e, f) 410°C × 64 h

at 410 °C×32 h, β-$Mg_{17}Al_{12}$ phase disappears and only Al_2Ca phase is observed at grain boundaries. When the holding time for T4 treatment is further increased to 64 h, there is still a large amount of Al_2Ca phase at grain boundaries, which confirms the high thermal stability of Al_2Ca phase at 410 °C. Although the dissolution of Al_2Ca phase is hard to realize during T4 treatment at 410 °C, the morphology of lamellar Al_2Ca phase changes obviously with the extending of holding time. The connected network-like Al_2Ca phase tends to separate gradually and the tips of Al_2Ca phase is partially spheroidized. However, the coarsening of α-Mg grains is not observed yet. It is because the existence of a large amount of Al_2Ca phase with high thermal stability at grain boundary regions is able to inhibit the grain growth during T4 treatment at 410 °C.

Figure 3 shows the quantitative metallographic analysis result about the content of second phases under different T4 treatment conditions. In the as-cast AZX912 alloy, the relative volume fraction of second phases is about 15.3%. After T4 treatment for 410 °C×32 h, the relative volume fraction of second phases decreases to about 9.2%. After T4 treatment for 410 °C×64 h, the relative volume fraction of second phases is about 9.1%. It is found that relative volume fractions of second phases in AZX912 alloy after T4 treatment for 410 °C×32 h and 410 °C×64 h are close to each other. These results are in accordance with the results in XRD analysis and microstructure characterization, indicating that the extended holding time from 32 h to 64 h has little effect on phase constitution of AZX912 alloy during T4 treatment at 410 °C.

Figure 4 shows the image mapping results of the distribution of Al and Ca elements in AZX912 alloy after T4 treatment for

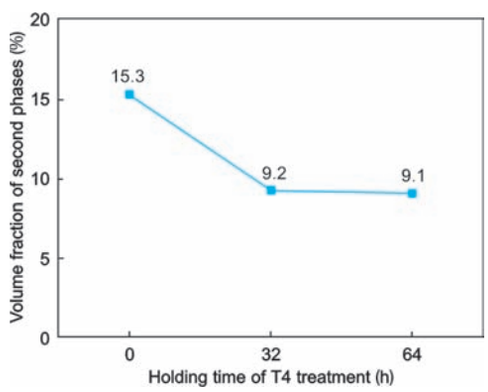

Fig. 3: Effect of holding time on relative volume fraction of second phases in AZX912 alloy under T4 treatment conditions

410 °C×32 h and 410 °C×64 h, respectively. Due to the high thermal stability of Al_2Ca phase, after T4 treatment for 410 °C×32 h, Ca element still mainly exists in Al_2Ca phase. Further increase the holding time to 64 h, the distribution of Ca element changes little. Comparatively, after T4 treatment at 410 °C for a longer time, except for Al element in Al_2Ca phase, the residual Al element tends to distribute uniformly in the matrix.

Figure 5 shows the bright field (BF) images and corresponding selected area electron diffraction (SAED) patterns of AZX912 alloy after T4 treatment for 410 °C×64 h. It is observed from Fig. 5(a) that the tips of second phase are round. The diffraction patterns in Fig. 5(b) are indexed as [112] zone axis patterns of face-centered cubic (FCC) structure. The lattice parameter is calculated to be a=0.8192 nm, which is very close to Al_2Ca phase (a=0.8038 nm). Therefore, the second phase is confirmed as Al_2Ca phase.

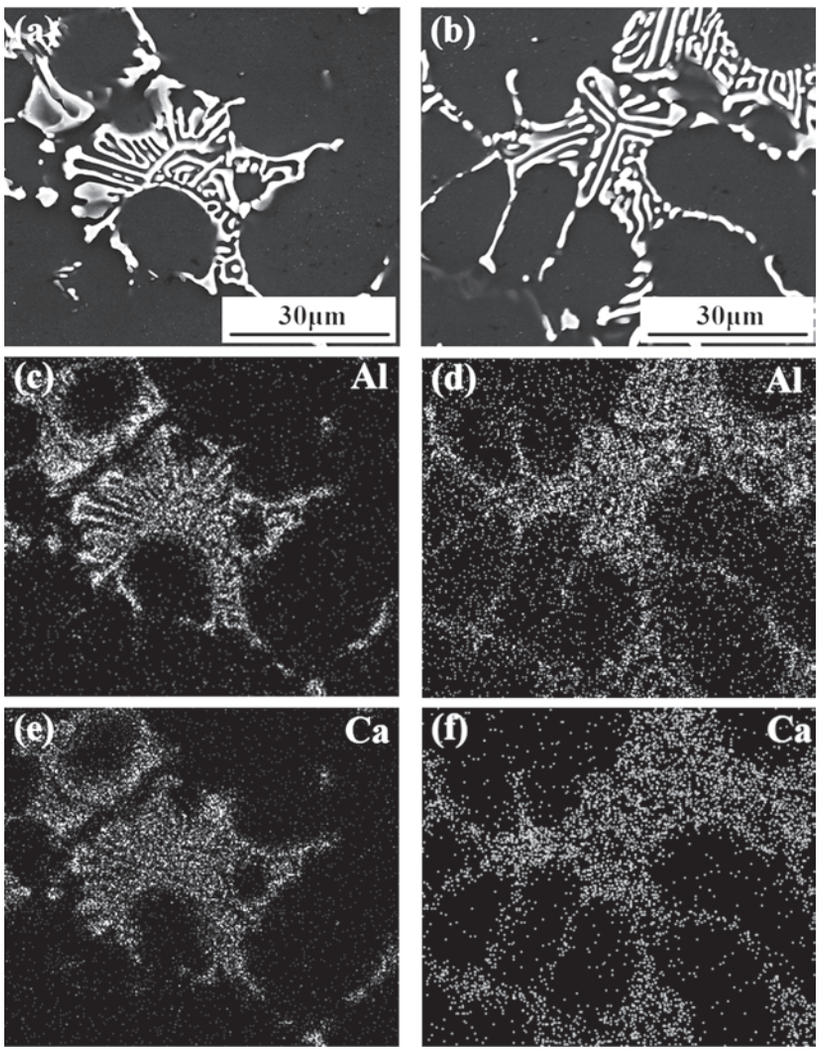

Fig. 4: Element mapping results of distribution of Al and Ca elements in AZX912 alloy after T4 treatment: (a, c, e) 410 °C × 32 h and (b, d, f) 410 °C × 64 h

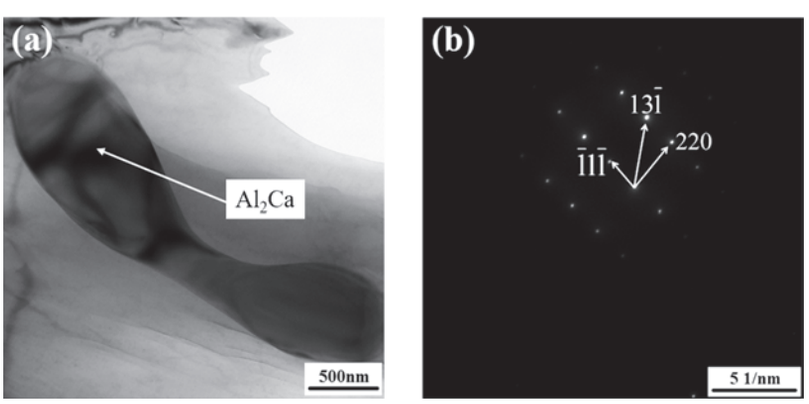

Fig. 5: TEM analysis of AZX912 alloy after T4 treatment for 410 °C × 64 h: (a) morphology and (b) diffraction pattern

Figure 6 presents the effect of T4 treatment conditions on mechanical properties of AZX912 alloy. The ultimate tensile strength (UTS), yield strength (YS) and elongation (E_f) of as-cast AZX912 alloy are 110.2 MPa, 177.9 MPa and 3.3%, respectively. With the extending of holding time during T4 treatment, the UTS and E_f of AZX912 alloy increase continuously and its YS decreases gradually. After T4 treatment for 410 °C×64 h, the YS, UTS and E_f of AZX912 alloy are 89.8 MPa, 199.7 MPa and 5.3%, respectively. Compared to as-cast AZX912 alloy sample, YS decreases by 18.5% while the UTS and E_f increase by 12.2% and 60.6%, respectively.

Figure 7 shows the age hardening curve of AZX912 alloy during isothermal ageing at 225 °C after T4 treatment for 410 °C×64 h. During isothermal ageing at 225 °C, the variation of hardness is not significant. With the prolongation of holding time, the hardness increases slowly and reaches the ageing peak at 96 h. The average

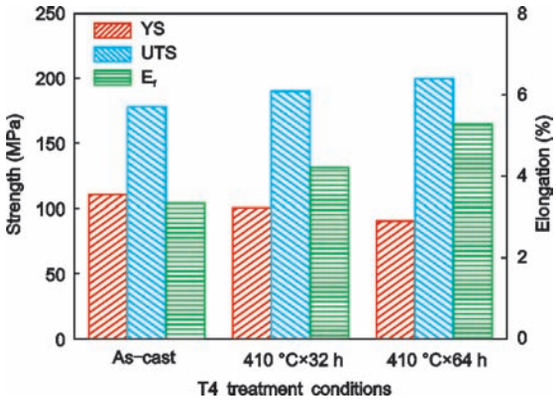

Fig. 6: Effect of T4 treatment conditions on mechanical properties of AZX912 alloy

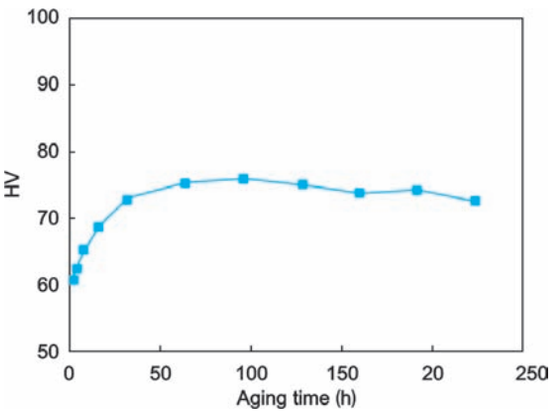

Fig. 7: Age hardening curve of AZX912 alloy during isothermal ageing at 225 °C after T4 treatment for 410 °C × 64 h

hardness increases from 61.2 HV at 0 h to 76.4 HV at 96 h and the increasing range is 24.8%. Further increase of ageing time brings the slight decrease of hardness and the average hardness slightly decreases to 72.1 HV after isothermal ageing at 225 °C for 224 h.

Figure 8 shows XRD patterns and analysis results of AZX912 alloy under different T6 treatment conditions. According to XRD results, during T6 treatment, β-$Mg_{17}Al_{12}$ phase reforms in AZX912 alloy. With the prolongation of ageing time, diffraction peaks of α-Mg and Al_2Ca phases change little while those of β-$Mg_{17}Al_{12}$ phase enhances continuously, indicating the increasing precipitation of β-$Mg_{17}Al_{12}$ phase during isothermal ageing at 225 °C.

Figure 9 shows the microstructures of AZX912 alloy under different T6 treatment conditions. As shown in Fig. 9(a, b), after

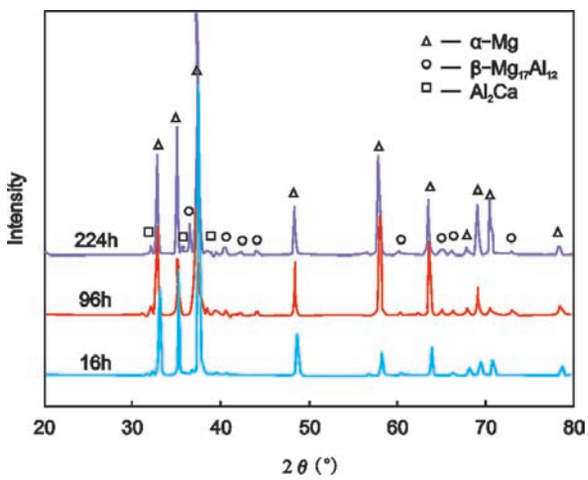

Fig. 8: XRD patterns of AZX912 alloy under different T6 treatment conditions

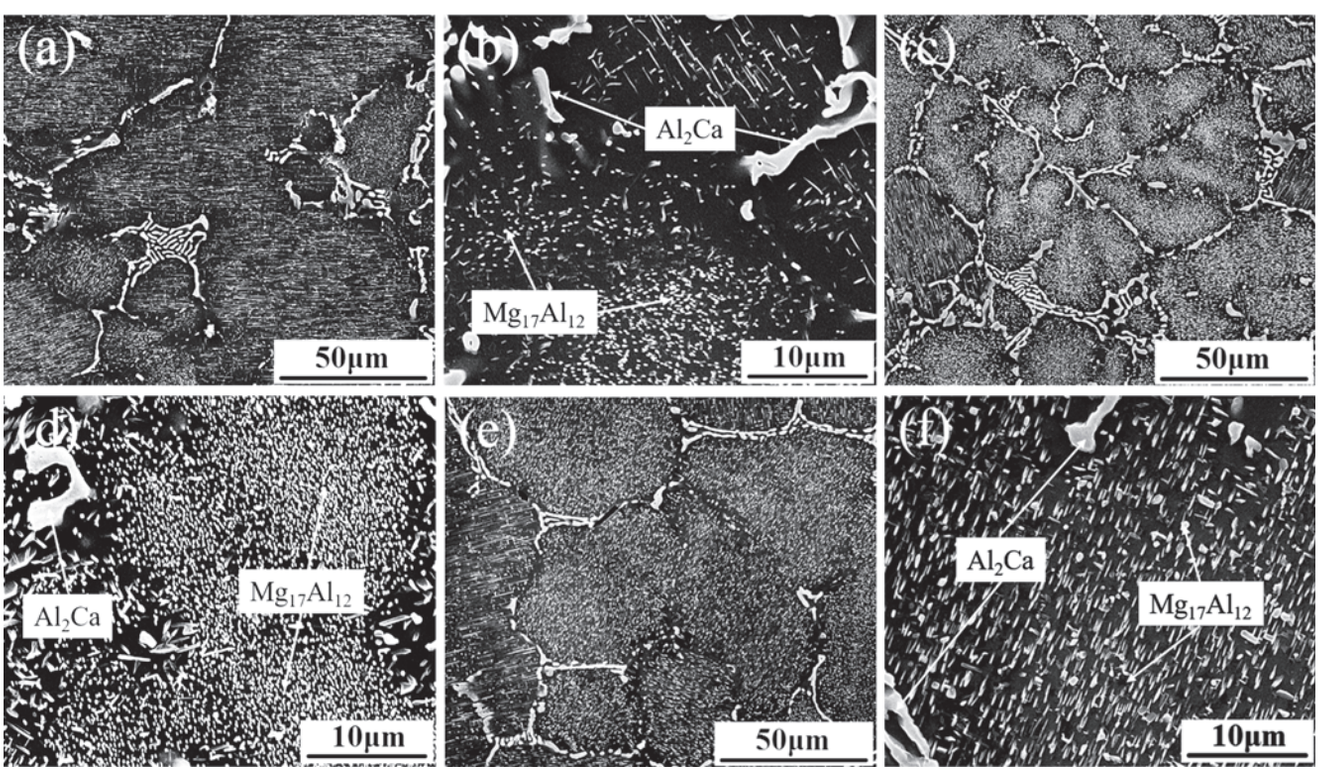

Fig. 9: SEM images of AZX912 alloy under different T6 treatment conditions: (a, b) 225 °C × 16 h; (c, d) 225 °C × 96 h and (e, f) 225 °C × 224 h

T6 treatment for 225 °C×16 h, a large amount of β-$Mg_{17}Al_{12}$ phase precipitates in the matrix. The precipitated β-$Mg_{17}Al_{12}$ phase is needle-like and small in size. According to the age hardening curve, AZX912 alloy reaches ageing peak when the ageing time increases to 96 h. The density of precipitated β-$Mg_{17}Al_{12}$ phase further increases while the coarsening in size is unobvious. However, after T6 treatment for 225 °C×224 h, the density of precipitated β-$Mg_{17}Al_{12}$ phase decreases compared to sample after T6 treatment for 225 °C×96 h and the coarsening of precipitated β-$Mg_{17}Al_{12}$ phase is significant.

Table 1 lists the mechanical properties of AZX912 alloy under the peak ageing condition (225 °C × 96 h). Under the peak ageing condition, YS of AZX912 alloy reaches 143.8 MPa, which is 60.1% higher than the sample after T4 treatment for 410 °C×64 h. However, its E_f decreases to only 1.8%, which is 66.0% lower than the sample after T4 treatment for 410 °C×64 h. Due to the deterioration of plasticity, there is little difference in UTS of peak ageing sample and the sample after T4 treatment for 410 °C× 64 h.

Table 1: Mechanical properties of AZX912 alloy under peak ageing condition (225 °C × 96 h)

Yield strength (YS, MPa)	Ultimate tensile strength (UTS, MPa)	Elongation (E_f, %)
143.8	198.0	1.8

According to the thermal analysis results by Liang et al [16], during the solidification of AZX912 alloy, Al_2Ca phase forms at 514 °C and β-$Mg_{17}Al_{12}$ phase forms at 427 °C. Therefore, during T4 treatment at 410 °C, only β-$Mg_{17}Al_{12}$ phase with low melting point would dissolve into the matrix while Al_2Ca phase with high melting point would not dissolve. However, it is found that, T4 treatment at 410 °C promotes the morphology modification of Al_2Ca phase in AZX912 alloy. The solute concentration at the interface between α-Mg matrix and Al_2Ca phase varies with the curvature radius, which provides the driving force for element diffusion. Due to the effect of surface tension, internal stress is produced where the curvature radius is small, leading to the increase of free energy. Therefore, the diffusion activation energy of atoms decreases and the diffusion is easy to take place [17].

The equilibrium concentration of alloying element in the matrix at the interface between second phase and the matrix can be established as:

$$\ln\frac{C_r}{C_\infty}=\frac{2M\sigma}{RT\rho r} \quad (1)$$

where C_r and C_∞ are the equilibrium concentration of solute element in the matrix where curvature radiuses are r and ∞, respectively, in the interface between second phase and the matrix, M is the relative molecular mass of second phase, σ is the interfacial tension between second phase and the matrix and ρ is the density of the matrix.

According to equation (1), the solute concentration increases with the decrease of r. A hypothesis is proposed here to explain the evolution of Al_2Ca phase during T4 treatment. Since the tips of lamellar Al_2Ca phase have a small curvature radius, the solute concentration in α-Mg matrix near the tips of Al_2Ca phase is higher than the rest. At elevated temperatures, alloying elements would diffuse from the tips to the flat region and destroy the equilibrium of the interface. The solute concentration in α-Mg matrix near the tips of Al_2Ca phase becomes unsaturated while that near the flat region becomes supersaturated. In order to restore balance, the tips of Al_2Ca phase dissolve with the increase of curvature radius while the flat region grows with the decrease of curvature radius, which might be the reason for partial spheroidization of Al_2Ca phase during T4 treatment.

It is also found in this study that with the prolongation of holding time during T4 treatment, YS of AZX912 alloy decreases gradually while UTS and E_f increase continuously. Due to the dissolution of β-$Mg_{17}Al_{12}$ phase during the T4 treatment, the hindering effect against dislocation movement during deformation is weakened and therefore YS is reduced. However, the dissolution and modification of brittle second phases can prevent stress concentration and inhibit the initiation and development of cracks, which is obviously beneficial to the plasticity. For the increase in the UTS, it is presumed that it comes from the contribution of the further release of the work-hardening potential due to the improvement in plasticity.

The solid solubility of Al in Mg is 12.6wt.% at 437 °C and it decreases to only 1.5wt.% at room temperature. Therefore, Al element would precipitate from the matrix during isothermal ageing. During T6 treatment, β-$Mg_{17}Al_{12}$ phase precipitates from supersaturated α-Mg matrix directly, without the formation of metastable phase [18]. In this study, the hardness of peak ageing sample is increased by about 24.8% compared to the sample after T4 treatment for 410 °C×64 h, which is lower than conventional AZ91 alloy. The relatively small increase in hardness of AZX912 alloy during isothermal ageing is because that a large amount of Al element exists in the form of Al_2Ca phase in AZX912 alloy. Al element in Al_2Ca phase with high thermal stability has no contribution to subsequent age hardening process. However, in conventional AZ91 alloy, except for Al element dissolved in the matrix, most of Al element precipitates in the form of β-$Mg_{17}Al_{12}$ phase. Therefore, the increase in hardness of ageing peak AZX912 alloy is not as significant as AZ91 alloy [19].

For conventional AZ91 alloy, the holding temperature for isothermal ageing is usually set at 200 °C, while the holding temperature is increased to 225 °C in this study. However, even aged at 225 °C, it takes 96 h for AZX912 alloy to reach peak ageing condition, while the ageing peak time for AZ91 alloy is only 16 h at 200 °C. The substantially extended time for ageing peak of AZX912 alloy is due to the existence of Ca element. Except for Ca element in Al_2Ca phase, there is still a part of Ca element dissolved in the matrix. The dissolved Ca element inhibits the quick precipitation of β-$Mg_{17}Al_{12}$ phase and therefore the peak-aged condition is delayed. From another

point of view, it is beneficial to enhance the thermal stability of AZ91 alloy [20]. It can also be concluded from this study that, although the precipitation of β-$Mg_{17}Al_{12}$ phase can significantly improve YS of AZX912 alloy, its negative effect on plasticity severely restricts the improvement in comprehensive mechanical properties.

3 Conclusions

AZX912 alloy was prepared by RSC process and then subjected to heat treatment. The effects of solid solution and isothermal ageing on microstructure evolution and mechanical properties of AZX912 alloy were studied. Following conclusions can be drawn:

(1) During T4 treatment at 410 °C, β-$Mg_{17}Al_{12}$ phase dissolves and undissolved Al_2Ca phase changes from connected network-like to partially spheroidized. The morphology modification of Al_2Ca phase is due to the element diffusion driven by curvature radius.

(2) With the extended holding time during T4 treatment, yield strength of AZX912 alloy decreases gradually while the ultimate tensile strength and elongation increase continuously. The decrease in yield strength and increase in E_f are due to the dissolution and modification of brittle second phases. The increase in UTS comes from the contribution of the further release of the work-hardening potential due to the improvement in plasticity.

(3) T6 treatment at 225 °C promotes the precipitation of β-$Mg_{17}Al_{12}$ phase after T4 treatment for 410 °C×64 h. The hardness reaches the peak after 96 h and the increase in hardness is about 24.8%. The precipitation of β-$Mg_{17}Al_{12}$ phase can significantly improve yield strength of AZX912 alloy, but its negative effect on plasticity severely restricts the improvement in comprehensive mechanical properties.

References

[1] Kabirian F, Mahmudi R. Effects of Rare Earth Element Additions on the Impression Creep Behavior of AZ91 Magnesium Alloy. Metall Mater Trans A, 2009, 40: 2190–2201.
[2] Cheng Suling, Yang Gencang, Fan Jianfeng, et al. Effect of Ca and Y additions on oxidation behavior of AZ91 alloy at elevated temperatures. Trans Nonferrous Met Soc China, 2009, 19: 299–304.
[3] Amberger D, Eisenlohr P, Göken M. Microstructural evolution during creep of Ca-containing AZ91. Mater Sci Eng A, 2009, 510: 98–402.
[4] Amberger D, Eisenlohr P, Göken M. On the importance of a connected hard-phase skeleton for the creep resistance of Mg alloys. Acta Mater, 2012, 60: 2277–2289.
[5] Wu Guohua, Fan Yu, Gao Hongtao, et al. The effect of Ca and rare earth elements on the microstructure, mechanical properties and corrosion behavior of AZ91D. Mater Sci Eng A, 2005, 408: 255–63.
[6] Fan Z. Semisolid metal processing. Int Mater Rev, 2002, 47: 49–85.
[7] Wu Shusen, Lü Shulin, An Ping, et al. Microstructure and property of rheocasting aluminum-alloy made with indirect ultrasonic vibration process. Mater Lett, 2012, 73: 150–153.
[8] Dai Wei, Wu Shusen, Lü Shulin, et al. Effects of rheo-squeeze casting parameters on microstructure and mechanical properties of AlCuMnTi alloy. Mater Sci Eng A, 2012, 538: 320–326.
[9] Lü Shulin, Wu Shusen, Dai Wei, et al. The indirect ultrasonic vibration process for rheo-squeeze casting of A356 aluminum alloy. J Mater Process Technol, 2012, 212: 1281–1287.
[10] Mahathaninwong N, Plookphol T, Wannasin J, et al. T6 heat treatment of rheocasting 7075 Al alloy. Mater Sci Eng A, 2012, 532: 91–99.
[11] Esgandari B A, Mehrjoo H, Nami B, et al. The effect of Ca and RE elements on the precipitation kinetics of $Mg_{17}Al_{12}$ phase during artificial aging of magnesium alloy AZ91. Mater Sci Eng A, 2011, 528: 5018–5024.
[12] Wang Qudong, Chen Wenzhou, Zeng Xiaoqin, et al. Effects of Ca addition on the microstructure and mechanical properties of AZ91magnesium alloy. J Mater Sci, 2001, 36: 3035–3040.
[13] Zhang Yang, Wu Guohua, Liu Wencai, et al. Microstructure and mechanical properties of rheo-squeeze casting AZ91-Ca magnesium alloy prepared by gas bubbling process. Mater Des, 2015: 67: 1–8.
[14] Xue Feng, Ming Xuegang, Sun Yangshan. Microstructures and mechanical properties of AZ91 alloy with combined additions of Ca and Si. J Mater Sci, 2006, 41: 4725–4731.
[15] Zhang Yang, Wu Guohua, Liu Wencai, et al. Preparation and rheo-squeeze casting of semi-solid AZ91-2wt.%Ca magnesium alloy by gas bubbling process. J Mater Res, 2015, 30: 825–832.
[16] Liang S M, Chen R S, Blandin J J, et al. Thermal analysis and solidification pathways of Mg-Al-Ca system alloys. Mater Sci Eng A, 2008, 480: 365–372.
[17] Zhang Jumei, Wang Zhihu, Jiang Bailing, et al. Influence of annealing and spheroidizing treatment on microstructure and mechanical properties of AZ91 magnesium alloy. China Foundry, 2013, 10: 34–38.
[18] Wang Zhiwei, Yan Hong, Huang Wenxian. Effect of solution treatment on microstructure and hardness of rheo-forming AZ91-Y alloy. China Foundry, 2016, 13: 383–388.
[19] Caceres C H, Davidson C J, Griffiths J R, et al. Effects of solidification rate and ageing on the microstructure and mechanical properties of AZ91 alloy. Mater Sci Eng A, 2002, 325: 344–355.
[20] Srinivasan A, Pillai U T S, Pai B C. Effects of elemental additions (Si and Sb) on the ageing behavior of AZ91 magnesium alloy. Mater Sci Eng A, 2010, 527: 6543–6550.

This work was financially supported by National Natural Science Foundation of China (No. 51601076 and No. 51401093) and Natural Science Fund for Colleges and Universities in Jiangsu Province (No. 16KJB430013).